

## HAWC measurements on the total energy spectrum of cosmic rays

**J. A. Morales-Soto<sup>a,\*</sup> and J. C. Arteaga-Velázquez<sup>a</sup> for the HAWC collaboration**

<sup>a</sup>*Instituto de Física y Matemáticas,*

*Universidad Michoacana de San Nicolás de Hidalgo, Morelia, Mexico*

*E-mail: [jorge.morales@umich.mx](mailto:jorge.morales@umich.mx), [juan.arteaga@umich.mx](mailto:juan.arteaga@umich.mx)*

To fully comprehend the nature of the propagation and acceleration mechanisms of TeV cosmic rays it is essential to study their energy spectrum with great precision and high statistics. To this matter a new generation of cosmic-ray experiments, like the HAWC observatory, has been built to enable unprecedented measurements of the cosmic-ray spectrum at TeV energies. In this work, we present a measurement of the total energy spectrum of cosmic rays from 10 TeV up to 1 PeV using HAWC. The events were collected from January 2017 to December 2020. CORSIKA/QGSJET-II-04 simulations were employed to estimate the energy of the cosmic-ray primaries. In this study we applied the Bayes' unfolding method on the measured air-shower energy distribution of the data in order to obtain the all-particle cosmic-ray energy spectrum. We found that the spectrum shows a break at  $(28.1^{+1.3}_{-1.2})$  (stat) TeV with a statistical significance of at least  $4.2 \sigma$ . At this energy the spectral index changes from  $\alpha_1 = -2.41 \pm 0.01$  (stat) to  $\alpha_2 = -2.73 \pm 0.01$  (stat). Our result is consistent with previous reports about the presence of a spectral break.

38th International Cosmic Ray Conference (ICRC2023)  
26 July - 3 August, 2023  
Nagoya, Japan



---

\*Speaker

## 1. Introduction

What's the origin of cosmic rays and what are their acceleration and propagation mechanisms? These questions have been in the air since the discovery of this radiation more than 100 years ago and, although nowadays there are many different astrophysical models based on theory and experimental results (see for example [1–4]) that try to provide some answers, the mystery has not been fully resolved. Some clues to answer the above questions may be found in the energy spectrum of cosmic rays. In the recent years, experiments like ATIC-02 [5], ARGO [6], CREAM [7], DAMPE [8], GRAPES-3 [9], HAWC [10], NUCLEON [11], and TIBET [12], have contributed to the measurement of the total cosmic-ray energy spectrum in different energy regimes. In particular, HAWC's measurement reveals the existence of a new break at tens of TeV. This result is supported by the observations made by NUCLEON, that also show a bend in the energy spectrum in the same energy regime.

The High Altitude Water Cherenkov (HAWC) observatory is an experiment specifically designed for the measurement of gamma rays and cosmic rays at TeV energies. Its main array is made up of 300 water Cherenkov tanks filled up with ultra pure water (60 ML of water in total), distributed over a flat area of 22000 m<sup>2</sup>, and located at the slope of the Sierra Negra, Puebla, Mexico, at an altitude of 4100 m above sea level. Each Cherenkov detector has 4 photomultipliers (PMTs) deployed at the bottom of the instrument, giving a total of 1200 in the array. Related to cosmic-ray studies, the HAWC collaboration has contributed with the measurement of the total energy spectrum in the energy region from 10 to 500 TeV [10] and of the energy spectrum of the mass group of H+He from 6 to 158 TeV [13].

This particular study provides an updated result on the all-particle cosmic ray energy spectrum measured by HAWC, extending the measurements up to 1 PeV and improving the estimation of the statistical and systematic uncertainties. We reconstructed the total spectrum by the implementation of an unfolding algorithm based on the Bayes theorem [14–16], which was applied to an experimental HAWC data sample with 3.8 years of effective time.

## 2. HAWC simulations and data sets

For the reconstruction of the energy spectrum and to study the systematic errors of the result we made use of MC simulations generated with CORSIKA (v760) [17]. Given the need to focus this work, we will only focus in the most relevant steps in the generation of the simulations, for more details and information the reader is referred to [13, 18]. To start with, low energy cosmic ray air shower events ( $E < 80$  GeV) and hadronic interactions with higher energies ( $E \geq 80$  GeV) were generated with CORSIKA, making use of the hadronic interaction models FLUKA [19] and QGSJet-II-04 [20], respectively. To reproduce how the incoming shower's particles interact with HAWC's Cherenkov detectors we made use of GEANT4 [21]. In total there are 8 species simulated in the MC data (H, He, C, O, Ne, Mg, Si and Fe) with an  $E^{-2}$  differential energy spectrum and arrival directions in the zenith angle range  $\theta = [0^\circ, 65^\circ]$ . The MC simulations were weighted to have a broken power law spectra according to a cosmic-ray composition model obtained from fits to direct measurements [7, 22–25]. Since protons are the most abundant nuclei in the TeV region, the simulations for these primaries were employed for the energy calibration procedure of the data

which is based on a log-likelihood analysis that compares probability tables generated for protons of different energies, charge distributions and zenith angle intervals using QGSJET-II-04 with the experimental events. The HAWC data that we selected for this work were measured during the time period between January 1, 2017 and December 31, 2020. To reduce the effect of systematic errors in our study, we only selected events that were successfully reconstructed (according to the procedure detailed in [18]), with zenith angles smaller or equal to  $35^\circ$ , that activated a minimum of 60 photomultipliers (PMTs) within a radius of 40 m from the core of the event and produced signal in more than 30% of the active PMT at the moment of the detection. Finally, those events that have the shower core mainly inside HAWC's physical area were selected. The energy, angular and shower core resolutions were estimated via MC simulations, resulting in 29%,  $0.5^\circ$ , and 11.8 m, respectively at  $E = 1$  PeV. After applying the selection cuts to the experimental data, we had a total of  $5.6 \times 10^{10}$  shower events.

### 3. Reconstruction procedure of the energy spectrum

We start our analysis by the reconstruction of the energy distribution,  $N(E_{rec})$ , from our measured data (see Fig. 1). We then proceed to correct the energy distribution for migration effects, this will grant us a more reliable result of the reconstruction of the energy spectrum. For this task, we implemented an unfolding method based on the Bayes theorem [14–16], where we make use of a response matrix,  $P(E_{rec}|E)$ , which is derived from MC simulations (see Fig. 2, left).

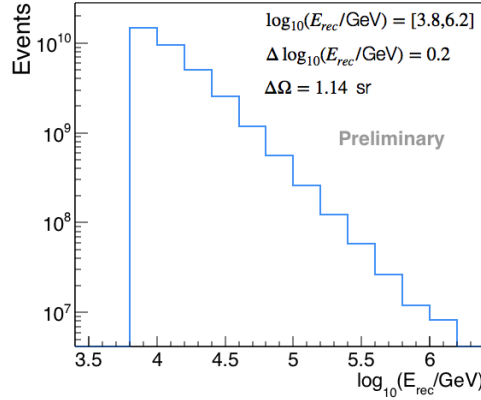


**Figure 1:** Energy distribution histogram,  $N(E_{rec})$ , derived from the selected data after the event selection criteria (see section 2).

Now that we have the unfolded energy spectrum,  $N(E)$ , from the experimental data, we are almost ready to reconstruct the energy spectrum, but we need one more element, the effective area (see Fig. 2, right), which is estimated from MC data as follows [10]:

$$A_{\text{eff}}(E) = A_{\text{thrown}} \cdot \epsilon(E), \quad (1)$$

where  $\epsilon(E)$  is the efficiency for detecting a shower event with true energy  $E$ , and  $A_{\text{thrown}}$  is the simulated throwing area, which has been projected and averaged over the solid angle.

Finally, the total energy spectrum of cosmic rays is reconstructed with the following formula:

$$\Phi(E) = \frac{N(E)}{\Delta E T \Delta\Omega A_{\text{eff}}}, \quad (2)$$

where  $\Delta E$  is the bin width of the energy distribution,  $T$  is the total effective time of observation, which corresponds to 3.8 years for this work, and  $\Delta\Omega$  is the differential solid angle.

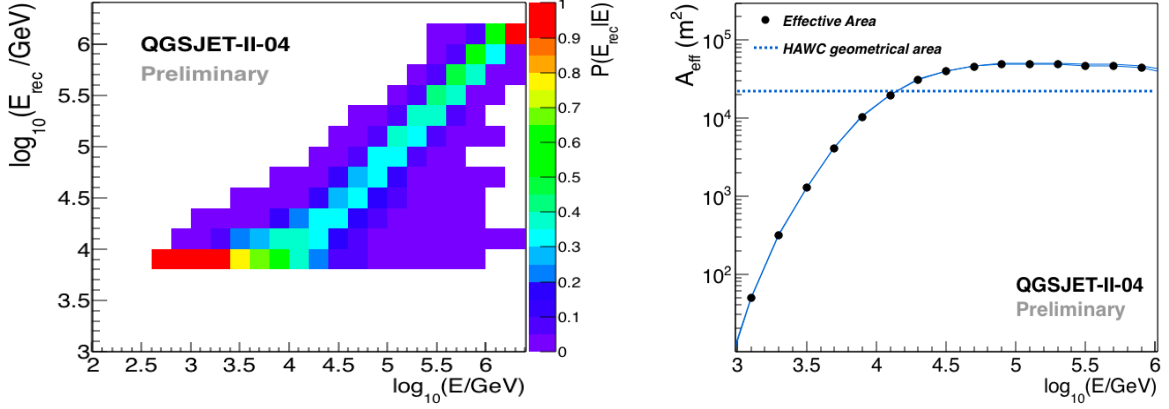


**Figure 2:** *Left:* The response matrix,  $P(E'|E)$ , that is used in our analysis was estimated from the simulations described in section 2. *Right:* Effective area as a function of the true primary energy,  $E$ . This quantity also comes from the MC simulations and it is used in the calculations for the reconstruction of the total energy spectrum. It is compared with HAWC’s physical area (dashed line).

### 3.1 Results

The main result from our analysis is shown in Fig. 3, left. In here, the energy spectrum is presented with its statistical errors (which include the limited statistics from both the data and the response matrix), and the systematic uncertainties. At bin  $\log_{10}(E/\text{GeV}) = 5.9$ , the statistical error is found between  $\pm 2.2\%$ , while the systematic uncertainties go from  $+10.3\%$  to  $-10.5\%$ . For this work, we covered the most relevant sources of systematic errors, like the effective area, and resolution of the PMTs, the late light effect and the charge resolution of the PMTs [18], the relative abundances of cosmic rays, the unfolding technique (by evaluating the dependence on the prior distribution and the smoothing algorithm, and by using Gold’s algorithm for the energy spectrum reconstruction [26]), and the differences between experimental runs (which were divided in intervals of one month). We found that the dominant sources of systematic errors at  $\log_{10}(E/\text{GeV}) = 5.9$  are the differences per run, the late light effect and the resolution of the PMTs.

As in [10], the observed total spectrum from Fig. 3 seems to follow a broken power-law rather than a power-law. We fitted our result inside the interval  $\log_{10}(E/\text{GeV}) = [4, 6]$  with both hypothesis and then compare the results by using a statistical analysis to see which scenario is preferred. For the analysis, as a test statistics we employed the difference of the chi-squares that are found for both fits. The power-law formula is given by

$$\Phi(E) = \Phi_0 E^{\gamma_1}, \quad (3)$$

where  $\Phi_0$  is a normalization parameter and  $\gamma_1$  is the spectral index. Likewise, the broken power law is defined as

$$\Phi(E) = \Phi_0 E^{\gamma_1} \left[ 1 + \left( \frac{E}{E_0} \right)^\epsilon \right]^{(\gamma_2 - \gamma_1)/\epsilon}, \quad (4)$$

where  $E_0$  is the position of the change in the spectral index,  $\gamma_1$  and  $\gamma_2$  are the spectral indexes before and after the break, and  $\epsilon$  is a parameter that measures the break's sharpness. For the fits we followed the  $\chi^2$ -minimization procedure described in [27], taking into account the statistical correlation between the measured points.

The fit results for the power-law scenario are  $\Phi_0 = 10^{4.31 \pm 0.01} \text{ m}^{-2} \text{ s}^{-1} \text{ sr}^{-1} \text{ GeV}^{-1}$  and  $\gamma_1 = -2.62 \pm 0.01$  with  $\chi_0^2 = 2059.31$  for a total of 8 degrees of freedom. On the other hand, the fit with the broken power-law formula gave  $\Phi_0 = 10^{3.46 \pm 0.03} \text{ m}^{-2} \text{ s}^{-1} \text{ sr}^{-1} \text{ GeV}^{-1}$ ,  $\gamma_1 = -2.41 \pm 0.01$ ,  $\gamma_2 = -2.73 \pm 0.01$ , and  $E_0 = (28.1_{-1.2}^{+1.3}) \text{ TeV}$  with  $\chi_1^2 = 10.38$  for 5 degrees of freedom.  $\epsilon$  was fixed to a value of 3. The observed test statistics is  $TS_{obs} = 2048.93$ . The next step was to obtain the  $TS$  distribution by assuming that the spectrum is best described by a power-law scenario. To do so we generated random toy spectra from a parent power-law distribution using the results of the fit with Eq. 4. We found no  $TS$  values above  $TS_{obs}$ , thus the  $p$ -value is less than  $1 \times 10^{-5}$ , which implies a significance of at least  $4.2 \sigma$  (stat) that the result is not described by the simple power-law hypothesis.

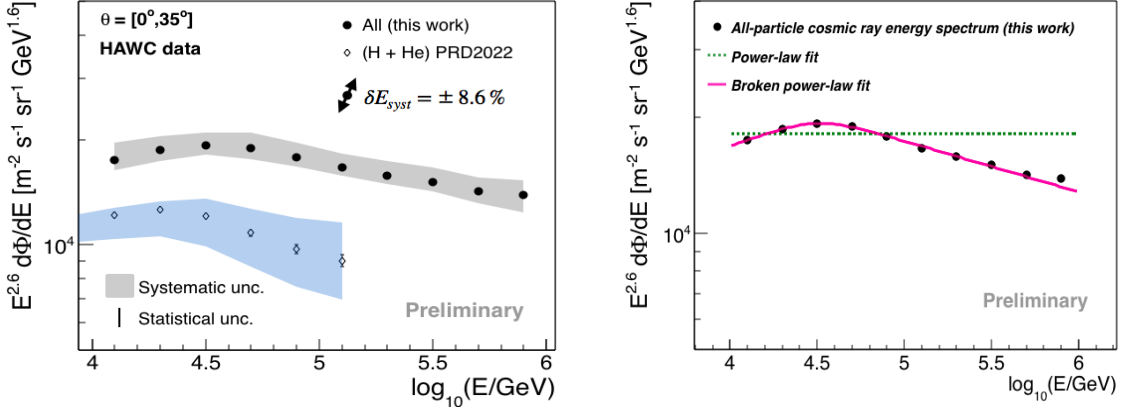


**Figure 3:** *Left:* The all-particle cosmic-ray energy spectrum measured by HAWC, unfolded from data taken during an effective time of 3.8 years (black dots). To better observe the shape of the spectrum, it is multiplied by an energy factor of  $E^{2.6}$ . Systematic uncertainties on the flux are represented by the gray error band, while the statistical errors are represented by bars. In this case, we compare our result to the one of the H + He component of cosmic rays from [13]. *Right:* HAWC's total energy spectrum (this work) fitted with the power-law formula from eq. (3) (green dotted line) and the broken power-law formula from eq. (4) (pink line).

Finally, we compared the spectrum obtained in this work to the results from other direct and indirect experiments in Fig. 4. For the comparison, we selected the measurements from ATIC-02 [5], NUCLEON [11], ARGO-YBJ [6], ICETOP [28], KASCADE [29, 30], TAIGA-HiSCORE [31], TIBET [12] and TUNKA-133 [32].

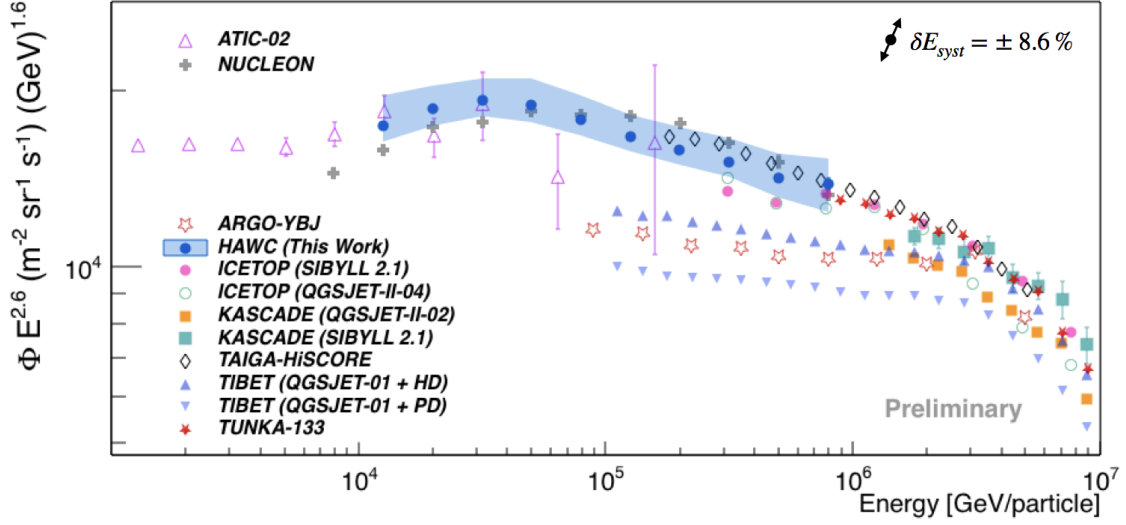


**Figure 4:** Comparison of the measurements of the spectrum from different cosmic-ray experiments (ATIC-02 (violet open triangles) [5], NUCLEON (red crosses) [11], ARGO-YBJ (violet crosses) [6], ICETOP (pink dots and green open circles) [28], KASCADE (orange squares and green squares) [29, 30], TAIGA-HiSCORE (green circles) [31], TIBET (upward blue triangles and downward blue triangles) [12] and TUNKA-133 (red stars) [32]) with our result of the HAWC all-particle energy spectrum of cosmic rays (black circles, this work).

#### 4. Discussion

In the present analysis, we have confirmed that the all-particle energy spectrum of cosmic rays is best described by a broken power-law in the energy range between 10 TeV and 1 PeV (see Fig. 3) with a significance of  $4.2 \sigma$ . This has also been observed in [11] and [10]. When comparing our result against other measurements (c.f. Fig. 4), we observe a good agreement with measurements from NUCLEON [11] within systematic errors. Also, at energies close to 10 TeV, HAWC’s data points are in agreement with ATIC-02 [5] data, and at energies closer to 1 PeV, our result is in agreement with TAIGA-HiSCORE [31] observations. On the other hand, HAWC’s measured energy spectrum is above the results from ARGO-YBJ [6], ICETOP [28], and TIBET [12]. In comparison to HAWC’s previous analysis [10], we reduced the systematic uncertainties of the HAWC energy spectrum. For example, at  $E = 100$  TeV, the systematic uncertainty was reduced from  $-24.8\%/+26.4\%$  to  $-5.5\%/+9.3\%$ . In Fig. 3, left, we compare the total spectrum with HAWC’s recent measurement of the H + He spectrum [13]. The later also shows evidence of a softening in the TeV region, specifically at 24 TeV. The fact that the feature in the total spectrum is located at higher energies than in the case of the spectrum of the light mass group could be due to the contribution of the heavy nuclei to the total intensity of cosmic rays.

## 5. Conclusions

HAWC's result on the all-particle energy spectrum from 10 TeV up to 1 PeV provide a bridge between direct and indirect measurements, along with the data from the NUCLEON satellite [11]. In this region the results of both experiments on the total spectrum of cosmic rays are in agreement within systematic uncertainties. For this work, we introduced an improved analysis of HAWC data on air showers induced by TeV cosmic rays, which allowed us to reconstruct the energy spectrum in the energy interval from 10 TeV up to 1 PeV. The present analysis on the all-particle energy spectrum shows a knee-like structure around 28 TeV with a significance of at least  $4.2\sigma$  (stat).

**Acknowledgments.** We acknowledge the support from: the US National Science Foundation (NSF); the US Department of Energy Office of High-Energy Physics; the Laboratory Directed Research and Development (LDRD) program of Los Alamos National Laboratory; Consejo Nacional de Ciencia y Tecnología (CONACyT), México, grants 271051, 232656, 260378, 179588, 254964, 258865, 243290, 132197, A1-S-46288, A1-S-22784, cátedras 873, 1563, 341, 323, Red HAWC, México; DGAPA-UNAM grants IG101320, IN111716-3, IN111419, IA102019, IN110621, IN110521; VIEP-BUAP; PIFI 2012, 2013, PROFOCIE 2014, 2015; the University of Wisconsin Alumni Research Foundation; the Institute of Geophysics, Planetary Physics, and Signatures at Los Alamos National Laboratory; Polish Science Centre grant, DEC-2017/27/B/ST9/02272; Coordinación de la Investigación Científica de la Universidad Michoacana; Royal Society - Newton Advanced Fellowship 180385; Generalitat Valenciana, grant CIDEAGENT/2018/034; Chulalongkorn University's CUniverse (CUAASC) grant; Coordinación General Académica e Innovación (CGAI-UdeG), PRODEP-SEP UDG-CA-499; Institute of Cosmic Ray Research (ICRR), University of Tokyo, H.F. acknowledges support by NASA under award number 80GSFC21M0002. We also acknowledge the significant contributions over many years of Stefan Westerhoff, Gaurang Yodh and Arnulfo Zepeda Dominguez, all deceased members of the HAWC collaboration. Thanks to Scott Delay, Luciano Díaz and Eduardo Murrieta for technical support.

## References

- [1] J. R. Hoerandel, *Astropart. Phys.* 21, 241 (2004).
- [2] S. Mollerach and E. Roulet, *Prog. Part. Nucl. Phys.* 98, 85 (2018).
- [3] M. Kachelriess, A. Neronov, and D. V. Semikoz, *Phys. Rev. D* 97, 063011 (2018).
- [4] V. I. Zatsepin and N. V. Sokolskaya, *Astron. Astrophys.* 458, 1 (2006); *Astron. Lett.* 33, 25 (2007).
- [5] A. D. Panov, J. H. Adams, et al. (2009). *Bulletin of the Russian Academy of Sciences: Physics*, 73(5), 564-567.
- [6] P. Montini, et al. *ArXiv*, preprint arXiv:1608.01389, 2016.
- [7] H. S. Ahn et al. (CREAM Collaboration), *Astrophys. J.* 707, 593 (2009).
- [8] Q. An, R. Asfandiyarov, et al. (2019). *Science advances*, 5(9), eaax3793.
- [9] F. Varsi, S. Ahmad, et al. (2019). *PoS (ICRC2019)*, 449.
- [10] R. Alfaro, and the HAWC Collaboration. *Physical Review D*, 96(12), 122001 (2017).
- [11] V. Grebenyuk, D. Karmanov, I. Kovalev, et al. *Advances in Space Research*, 64(12), 2546-2558 (2019).
- [12] M. Amenomori, X. Bi, et al., *The Astrophysical Journal*, vol. 678, no. 2, p. 1165, 2008.
- [13] J. C. Arteaga-Velázquez, J. D. Alvarez, and the HAWC Collaboration. *Physical Review D*, 105, 063021 (2022).
- [14] G. D'Agostini. *Nuclear Instruments and Methods in Physics Research Section A*, 362(2-3), 487-498 (1995).
- [15] W. H. Richardson (1972). *JoSA*, 62(1), 55-59.
- [16] L. B. Lucy (1974). *The astronomical journal*, 79, 745.
- [17] D. Heck, J. Knapp, J. N. Capdevielle, et al. Report FZKA 6019. Forschungszentrum Karlsruhe (1998).
- [18] A. U. Abeysekara, and the Hawc Collaboration. *The Astrophysical Journal*, 881(2), 134 (2019).
- [19] G. Battistoni, F. Cerutti, A. Fasso, et al. In *AIP Conference proceedings* Vol. 896, No. 1, pp. 31-49 (2007).
- [20] S. Ostapchenko. *Physical Review D*, 83(1), 014018 (2011).
- [21] S. Agostinelli, and the Geant4 Collaboration. *Nuclear instruments and methods in physics research section A*, 506(3), 250-303 (2003).

- [22] M. Aguilar et al. (AMS Collaboration), *Phys. Rev. Lett.* 114, 171103 (2015).
- [23] M. Aguilar et al. (AMS Collaboration), *Phys. Rev. Lett.* 115, 211101 (2015).
- [24] Y. S. Yoon et al. (CREAM Collaboration), *Astrophys. J.* 728, 122 (2011).
- [25] O. Adriani et al. (PAMELA Collaboration), *Science* 332, 69 (2011).
- [26] R. Gold. Report ANL-6984 (Argonne National Laboratory, USA, 1964).
- [27] P. A. Zyla et al. (Particle Data Group), *Prog. Theor. Exp. Phys.* 2020, 083C01 (2020) and 2021 update.
- [28] M. G. Aartsen, R. Abbasi, M. Ackermann, et al. *Physical Review D*, 102(12), 122001 (2020).
- [29] W. Apel, J. Arteaga-Velázquez, et al., *Astroparticle Physics*, vol. 47, pp. 54–66, 2013.
- [30] T. Antoni, W. Apel, et al., *Astroparticle physics*, vol. 24, no. 1-2, pp. 1–25, 2005
- [31] V. Prosin, I. Astapov, et al. (2019). *Bulletin of the Russian Academy of Sciences: Physics*, 83(8), 1016-1019.
- [32] V. Prosin, et al., *Nuclear Instruments and Methods in Physics Research Section A*, vol. 756, pp. 94–101, 2014.



## Full Authors List: Collaboration

A. Albert<sup>1</sup>, R. Alfaro<sup>2</sup>, C. Alvarez<sup>3</sup>, A. Andrés<sup>4</sup>, J.C. Arteaga-Velázquez<sup>5</sup>, D. Avila Rojas<sup>2</sup>, H.A. Ayala Solares<sup>6</sup>, R. Babu<sup>7</sup>, E. Belmont-Moreno<sup>2</sup>, K.S. Caballero-Mora<sup>3</sup>, T. Capistrán<sup>4</sup>, S. Yun-Cárcamo<sup>8</sup>, A. Carramiñana<sup>9</sup>, F. Carreón<sup>4</sup>, U. Cotti<sup>5</sup>, J. Cotzomi<sup>26</sup>, S. Coutiño de León<sup>10</sup>, E. De la Fuente<sup>11</sup>, D. Depaoli<sup>12</sup>, C. de León<sup>5</sup>, R. Díaz Hernandez<sup>9</sup>, J.C. Díaz-Vélez<sup>11</sup>, B.L. Dingus<sup>1</sup>, M. Durocher<sup>1</sup>, M.A. DuVernois<sup>10</sup>, K. Engel<sup>8</sup>, C. Espinoza<sup>2</sup>, K.L. Fan<sup>8</sup>, K. Fang<sup>10</sup>, N.I. Fraija<sup>4</sup>, J.A. García-González<sup>13</sup>, F. Garfias<sup>4</sup>, H. Goksu<sup>12</sup>, M.M. González<sup>4</sup>, J.A. Goodman<sup>8</sup>, S. Groetsch<sup>7</sup>, J.P. Harding<sup>1</sup>, S. Hernandez<sup>2</sup>, I. Herzog<sup>14</sup>, J. Hinton<sup>12</sup>, D. Huang<sup>7</sup>, F. Hueyotl-Zahuantitla<sup>3</sup>, P. Hüntemeyer<sup>7</sup>, A. Iriarte<sup>4</sup>, V. Joshi<sup>28</sup>, S. Kaufmann<sup>15</sup>, D. Kieda<sup>16</sup>, A. Lara<sup>17</sup>, J. Lee<sup>18</sup>, W.H. Lee<sup>4</sup>, H. León Vargas<sup>2</sup>, J. Linnemann<sup>14</sup>, A.L. Longinotti<sup>4</sup>, G. Luis-Raya<sup>15</sup>, K. Malone<sup>19</sup>, J. Martínez-Castro<sup>20</sup>, J.A.J. Matthews<sup>21</sup>, P. Miranda-Romagnoli<sup>22</sup>, J. Montes<sup>4</sup>, J.A. Morales-Soto<sup>5</sup>, M. Mostafá<sup>6</sup>, L. Nellen<sup>23</sup>, M.U. Nisa<sup>14</sup>, R. Noriega-Papaqui<sup>22</sup>, L. Olivera-Nieto<sup>12</sup>, N. Omodei<sup>24</sup>, Y. Pérez Araujo<sup>4</sup>, E.G. Pérez-Pérez<sup>15</sup>, A. Pratts<sup>2</sup>, C.D. Rho<sup>25</sup>, D. Rosa-Gonzalez<sup>9</sup>, E. Ruiz-Velasco<sup>12</sup>, H. Salazar<sup>26</sup>, D. Salazar-Gallegos<sup>14</sup>, A. Sandoval<sup>2</sup>, M. Schneider<sup>8</sup>, G. Schwefer<sup>12</sup>, J. Serna-Franco<sup>2</sup>, A.J. Smith<sup>8</sup>, Y. Son<sup>18</sup>, R.W. Springer<sup>16</sup>, O. Tibolla<sup>15</sup>, K. Tollefson<sup>14</sup>, I. Torres<sup>9</sup>, R. Torres-Escobedo<sup>27</sup>, R. Turner<sup>7</sup>, F. Ureña-Mena<sup>9</sup>, E. Varela<sup>26</sup>, L. Villaseñor<sup>26</sup>, X. Wang<sup>7</sup>, I.J. Watson<sup>18</sup>, F. Werner<sup>12</sup>, K. Whitaker<sup>6</sup>, E. Willcox<sup>8</sup>, H. Wu<sup>10</sup>, H. Zhou<sup>27</sup>

<sup>1</sup>Physics Division, Los Alamos National Laboratory, Los Alamos, NM, USA, <sup>2</sup>Instituto de Física, Universidad Nacional Autónoma de México, Ciudad de México, México, <sup>3</sup>Universidad Autónoma de Chiapas, Tuxtla Gutiérrez, Chiapas, México, <sup>4</sup>Instituto de Astronomía, Universidad Nacional Autónoma de México, Ciudad de México, México, <sup>5</sup>Instituto de Física y Matemáticas, Universidad Michoacana de San Nicolás de Hidalgo, Morelia, Michoacán, México, <sup>6</sup>Department of Physics, Pennsylvania State University, University Park, PA, USA, <sup>7</sup>Department of Physics, Michigan Technological University, Houghton, MI, USA, <sup>8</sup>Department of Physics, University of Maryland, College Park, MD, USA, <sup>9</sup>Instituto Nacional de Astrofísica, Óptica y Electrónica, Tonantzintla, Puebla, México, <sup>10</sup>Department of Physics, University of Wisconsin-Madison, Madison, WI, USA, <sup>11</sup>CUCEI, CUCEA, Universidad de Guadalajara, Guadalajara, Jalisco, México, <sup>12</sup>Max-Planck Institute for Nuclear Physics, Heidelberg, Germany, <sup>13</sup>Tecnologico de Monterrey, Escuela de Ingeniería y Ciencias, Ave. Eugenio Garza Sada 2501, Monterrey, N.L., 64849, México, <sup>14</sup>Department of Physics and Astronomy, Michigan State University, East Lansing, MI, USA, <sup>15</sup>Universidad Politécnica de Pachuca, Pachuca, Hgo, México, <sup>16</sup>Department of Physics and Astronomy, University of Utah, Salt Lake City, UT, USA, <sup>17</sup>Instituto de Geofísica, Universidad Nacional Autónoma de México, Ciudad de México, México, <sup>18</sup>University of Seoul, Seoul, Rep. of Korea, <sup>19</sup>Space Science and Applications Group, Los Alamos National Laboratory, Los Alamos, NM USA, <sup>20</sup>Centro de Investigación en Computación, Instituto Politécnico Nacional, Ciudad de México, México, <sup>21</sup>Department of Physics and Astronomy, University of New Mexico, Albuquerque, NM, USA, <sup>22</sup>Universidad Autónoma del Estado de Hidalgo, Pachuca, Hgo., México, <sup>23</sup>Instituto de Ciencias Nucleares, Universidad Nacional Autónoma de México, Ciudad de México, México, <sup>24</sup>Stanford University, Stanford, CA, USA, <sup>25</sup>Department of Physics, Sungkyunkwan University, Suwon, South Korea, <sup>26</sup>Facultad de Ciencias Físico Matemáticas, Benemérita Universidad Autónoma de Puebla, Puebla, México, <sup>27</sup>Tsung-Dao Lee Institute and School of Physics and Astronomy, Shanghai Jiao Tong University, Shanghai, China, <sup>28</sup>Erlangen Centre for Astroparticle Physics, Friedrich Alexander Universität, Erlangen, BY, Germany